Imaging in Sarcoidosis

Hilario Nunes, M.D.,[1] Pierre-Yves Brillet, M.D.,[2] Dominique Valeyre, M.D.,[1] Michel W. Brauner, M.D.,[2] and Athol U. Wells, M.D.[3]

ABSTRACT

Sarcoidosis is a multisystemic granulomatous disease of unknown etiology that may involve virtually any organ. Pulmonary involvement predominates, but sarcoidosis can involve multiple organs, with or without concomitant lung involvement. Aberrations on chest radiographs are present in more than 90% of patients with sarcoidosis. Bilateral hilar lymphadenopathy, with or without lung parenchymal infiltrates, is typical but a wide range of chest radiographic patterns may be observed. This article discusses the characteristic chest radiographic features of sarcoidosis and the prognostic value of the radiographic staging classification as espoused by Scadding more than 4 decades ago. Thin-section high-resolution computed tomographic (HRCT) scans more clearly elucidate the intrathoracic lesions observed in sarcoidosis and may discriminate active inflammation from end-stage fibrosis. Although HRCT is not necessary to manage all cases of sarcoidosis, HRCT may be invaluable in *selected* patients with stage II or III sarcoidosis to discriminate alveolitis (which may be amenable to therapy) from fibrosis. Additionally, radionuclide techniques may have a role in extrapulmonary sarcoidosis (particularly when central nervous system or cardiac involvement is suspected). We review the salient features and role of magnetic resonance imaging and diverse radionuclide techniques to diagnose or follow selected cases of extrapulmonary sarcoidosis.

KEYWORDS: Sarcoidosis, chest radiographs, computed tomographic (CT) scans, magnetic resonance imaging (MRI), radionuclide scans

Sarcoidosis is a multisystemic granulomatous disease of unknown etiology.[1–3] Multiple clinical phenotypes are observed as judged by the mode of presentation, pattern of organ involvement, disease duration, and severity. Sarcoidosis primarily affects the lungs and the lymphatic system in more than 90% of patients but virtually no organ is immune from the disease.[1–3] The diagnosis of sarcoidosis is based upon the association of compatible clinicoradiological findings, histological demonstration of noncaseating granulomas, and exclusion of other granulomatous disorders.[1] However, the clinical and radiological expression of the disease is remarkably variable, with findings sometimes pathognomonic but often merely suggestive or markedly atypical. The radiological differential diagnosis is often broad, and because histological confirmation is sometimes elusive, a confident diagnosis often requires the amalgamation of information from imaging and other tests. Moreover, chest radiographic findings make a major contribution to prognostic evaluation. The course and prognosis of sarcoidosis are highly variable.[1–3] Although spontaneous recovery occurs in nearly two thirds of cases, therapy is necessary in one third of cases, and some patients experience a prolonged and severe course.

[1]Services de Pneumologie; [2]Radiologie, Hôpital Avicenne, Assistance Publique-Hôpitaux de Paris, Université Paris, Bobigny, France; [3]Interstitial Lung Disease Unit, Royal Brompton Hospital, London, United Kingdom.

Address for correspondence and reprint requests: Hilario Nunes, M.D., Service de Pneumologie, Hôpital Universitaire Avicenne, 125 rue de Stalingrad, 93009 Bobigny, France. E-mail: hilario.nunes@avc.aphp.fr.

Sarcoidosis: Evolving Concepts and Controversies; Guest Editors, Marc A. Judson, M.D., Michael C. Iannuzzi, M.D.

Semin Respir Crit Care Med 2007;28:102–120.
DOI 10.1055/s-2007-970336. ISSN 1069-3424.

Adverse prognostic determinants applicable to small groups of patients include onset of the disease after the age of 40, neurosarcoidosis, cardiac involvement, lupus pernio, sinonasal involvement, chronic uveitis, chronic hypercalcemia, nephrocalcinosis, and bone involvement.[1–3] By contrast, chest radiograph staging is relevant to most patients, and in the remaining cases with a major extrapulmonic pattern of disease, imaging procedures at other sites are usually central to prognostic evaluation and the formulation of management.

This article reviews our current knowledge and the emerging concepts in the imaging of sarcoidosis, with a particular focus on pulmonary sarcoidosis and a broader review of other selected sites of involvement. The article describes both typical and atypical features and discusses the role of imaging as a diagnostic and prognostic tool in the management of patients with sarcoidosis.

PULMONARY SARCOIDOSIS—CHEST RADIOGRAPH

Despite the progress in new imaging technologies, conventional chest radiograph continues to have a crucial role for the diagnosis, prognosis, and follow-up of sarcoidosis. The chest radiograph is abnormal at some point in more than 90% of patients[1–5] and is often the first investigation to suggest the diagnosis. Up to 60% of patients present with asymptomatic chest radiographic abnormalities.[2,3]

Radiographic Staging

More than 4 decades ago, Scadding classified posteroanterior (PA) chest radiographic findings as stage 0 (a normal radiograph), stage I [bilateral hilar lymphadenopathy (BHL), variably associated with paratracheal adenopathy] (Fig. 1), stage II (BHL accompanied by parenchymal infiltration) (Fig. 2), stage III (parenchymal infiltration without BHL) (Fig. 3) and stage IV (parenchymal infiltration with overt pulmonary fibrosis) (Fig. 4).[1,6] The frequency of each stage at presentation is reported as stage 0: 8 to 16%, stage I: 25 to 65%, stage II: 14 to 49%, stage III: ~10%, stage IV: ~5%.[2]

Radiographic Features

Sarcoid lymphadenopathy is typically bilateral, symmetrical, and noncompressive.[3,7–9] The most characteristic feature is BHL, noted in 50 to 80%. In patients with thoracic lymphadenopathy, BHL is present in over 95% of cases, with enlargement of right paratracheal and aortic-pulmonic window lymph nodes also common (> 70%). Subcarinal (21%), anterior mediastinal (16%), and posterior mediastinal (2%) involvement are less frequent.[9] Lone paratracheal, subcarinal, or mediastinal

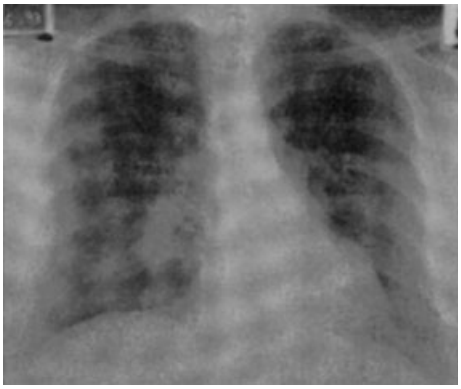

Figure 1 Radiographic stage I. The posteroanterior film shows bilateral noncompressive, predominantly right-sided hilar lymphadenopathy with clear lung fields.

enlarged lymph nodes without BHL increases the likelihood of an alternative diagnosis, particularly lymphoma. Lymph node size ranges from minimal to massive and tends to be largest at presentation, with gradual diminution leading, in a majority of cases, to complete regression within 2 years. In long-standing cases nodal eggshell calcification may be observed.

Parenchymal infiltration is noted in 25 to 50% of patients with sarcoidosis.[3] It is usually bilateral and symmetrical with a patent predominance for central regions and upper lobes. The pattern of infiltration is typically micronodular or reticulomicronodular.[2,3] Other well-recognized radiographic features, including focal alveolar opacities and ground-glass opacities, are less frequent. In progressive disease, radiological evidence of fibrosis becomes increasingly prominent, including architectural distortion, upper lobe volume loss with hilar retraction, masses, coarse linear bands, and bullae.[2,3] Findings are atypical in ~20% of cases[10,11] and are more frequent over the age of 50.[12]

Either the pattern or the distribution of disease may be abnormal.[10,11] Opacities may be basal or confined to part or all of one lung. Among a multiplicity of

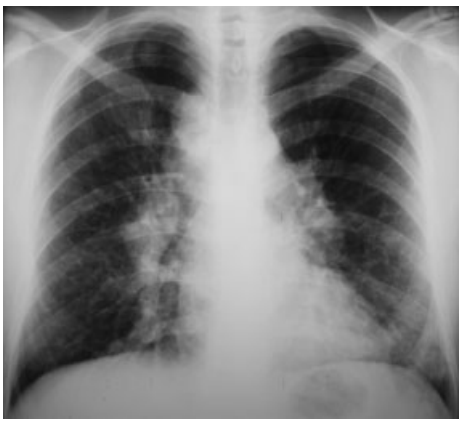

Figure 2 Radiographic stage II. The posteroanterior film shows symmetrical bilateral hilar lymphadenopathy associated with parenchymal infiltration.

Figure 3 Radiographic stage III. The posteroanterior film shows parenchymal infiltration without hilar lymphadenopathy, but no obvious fibrotic changes. The parenchymal shadowing is micronodular and has a predilection for the mid and upper parts of the lungs.

atypical patterns, the most frequent are multiple large, round nodules and alveolar consolidations, named "nodular"[13–15] or "alveolar sarcoidosis"[16]; diffuse ground-glass opacities[17]; tumorlike opacities[15]; cavitation[4,18]; pleural involvement, including effusion,[19] pleural thickening or calcification, and pneumothorax[20]; and atelectases.[21,22] These features may occur in isolation but are often admixed with more typical abnormalities.[10,11] Radiological atypical presentations and complications will be discussed in the section on computed tomography (CT) because CT tends to be especially helpful when the chest radiographic diagnosis is not immediately apparent.

Diagnostic Role of Chest Radiography

In the absence of histological confirmation, clinical and/or radiological features may be diagnostic in stage I (reliability of 98%) or stage II (89%), but are less accurate for patients with stage III (52%) or stage 0 (23%) disease.[1] Other important causes of BHL, all much less frequent than sarcoidosis, are infection (fungal or mycobacterial) and malignancy (lymphoma, bronchogenic carcinoma or extrathoracic carcinoma). In a large review by Winterbauer et al, symmetrical BHL was the mode of presentation in only 3.8% of lymphomas, 0.8% of bronchogenic carcinomas, and 0.2% of extrathoracic carcinomas.[8] Asymptomatic BHL, in association with an unremarkable physical examination or acute symptoms (i.e., uveitis, polyarthritis, or erythema nodosum), was strongly indicative of sarcoidosis. BHL indicated malignancy when associated with anemia, a pleural effusion or anterior mediastinal mass, peripheral lymphadenopathy, or hepatosplenomegaly.[8] Thus histological confirmation can reasonably be viewed as superfluous in many patients with stage I disease, provided that disease resolution is rapid and spontaneous.[1]

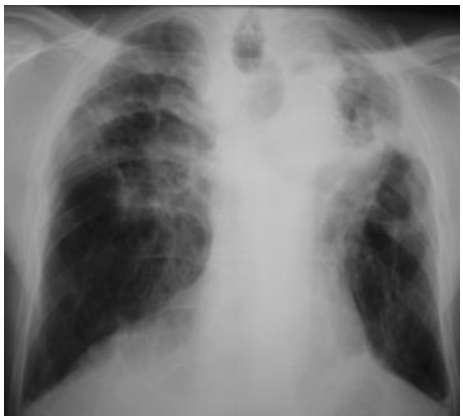

Figure 4 Radiographic stage IV. The posteroanterior film shows predominantly upper lobe fibrotic abnormalities with hilar retraction, coarse fibrotic masses (mostly on the left), and bibasal compensatory emphysema (secondary to the loss of upper lobe volume).

Prognostic Role of Chest Radiography

The purely descriptive nature of chest radiographic staging should be stressed. In individual cases, findings do not, in themselves, reliably discriminate between active inflammation and fibrosis, but they do identify major prognostic differences.[1–3,23–25] Spontaneous resolution occurs in 55 to 90% of patients with stage I, 40 to 70% with stage II, 10 to 20% with stage III, and does not occur with stage IV disease.[1–3,23–25] More than 85% of spontaneous remissions occur within the first 2 years and are very seldom followed by relapse. Regardless of the initial stage, the likelihood of remission is reduced after 2 years,[24] but changes in stage are highly variable. In a large patient cohort, only 9% of stage I patients had progressed to stage II (and 1.6% to stages III or IV) at 5 years, with only 5.5% of stage II patients progressing to stage IV.[25] Stage I persists after 5 years in up to 10% of cases, but this is not necessarily indicative of ongoing disease activity.[1–3]

Pulmonary function tests (PFTs) are abnormal in 20% of patients with stage I and 40 to 70% of patients with stage II, III, or IV, but functional impairment does not correlate well with chest radiographic changes.[1] Treatment is usually introduced because of symptoms or functional impairment but radiographic findings per se may also prompt therapeutic intervention.[26–28] A prospective randomized study conducted by the British Thoracic Society provides some support for long-term corticosteroid therapy in asymptomatic patients with radiographic abnormalities present for at least 12 months.[26] In another placebo-controlled study, patients with newly detected stage II or III disease and normal lung function indices were treated with oral prednisolone for 3 months, followed by inhaled budesonide for 15 months.[27] Radiographic benefits were maintained 5 years after cessation

of therapy but functional differences were small.[28] It remains uncertain whether modest improvements in asymptomatic patients justify the morbidity associated with treatment.

A further advantage of serial chest radiography is the detection of sarcoidosis complications, including pneumothorax, aspergilloma, bronchial stenosis, and pulmonary malignancy. In this regard, chest radiography often serves to prompt CT evaluation.

CHEST COMPUTED TOMOGRAPHY

Standard CT Scanning Protocols

HRCT is now widely accepted as the imaging reference standard in the evaluation of diffuse infiltrative lung diseases (DLDs).[29] HRCT is undoubtedly superior to conventional CT in delineating the distribution and pattern of pulmonary interstitial lesions. Collimation widths of 1 to 1.5 mm provide optimal signal. Thus, in routine diagnostic protocols, 1 to 1.5 mm thin slices are acquired at 10 mm spaced intervals from the apices to the bases at full inspiration.[29] For lung analysis, image reconstruction with a high-spatial-frequency algorithm enhances the definition of fine parenchymal detail.[29] Additional sections at end expiration may show air trapping in patients with small airways obstruction. Administration of contrast agents can be useful to better discern lymphadenopathy and in patients with vascular complications, including pulmonary hypertension (PH). Recently, the advent of multidetector CT (MDCT), combining helical volumetric acquisitions and thin slice thickness (0.6 to 1.25 mm), has allowed CT to image the entire lung during a single breath-hold. Postprocessing techniques are likely to become increasingly useful, especially maximum and minimum intensity projections, which enhance the detection and analysis of micronodular structures and areas of increased and reduced density.[30] However, MDCT acquisitions increase the radiation burden and the routine use of these new techniques has not been validated in young patients with sarcoidosis.

Indications for Chest CT

The role of CT in the diagnosis and management of sarcoidosis continues to be debated. The diagnostic accuracies of CT and chest radiography, with or without clinical information, have been compared in several studies of patients with a variety of DLDs.[31–36] When a confident diagnosis can be made from typical clinical and chest radiographic features, CT appears to add little,[1–3,37] especially in stage I disease. By contrast, HRCT makes important diagnostic contributions in selected cases with stage II, III, and IV.[1–3] According to the American Thoracic Society (ATS)/European Respiratory Society (ERS)/World Association of Sarcoidosis and Other Granulomatous Disorders (WASOG) expert consensus statement on sarcoidosis, CT can be justified in the following circumstances: (1) atypical clinical and/or chest radiograph findings, (2) a normal chest radiograph but a clinical suspicion of the disease, and (3) detection of complications of the lung disease.[1] CT findings may also discriminate between active inflammation and irreversible fibrosis,[38–44] with occasional influence on therapeutic decisions. Furthermore, numerous studies have explored correlations between disease severity on CT and functional impairment.[40,44–53] However, despite moderately strong functional morphological relationships in patient populations, HRCT makes only, at best, a small contribution to management in most individuals, once the diagnosis is secure.

The CT features of sarcoidosis have been extensively depicted in many studies[38–60] and have been the subject of several reviews.[61,62] The spectrum of disease on CT is extraordinarily variable. Several characteristic CT profiles have now been identified, but in many cases appearances are atypical and not strongly suggestive of the diagnosis.

Typical CT Features

THORACIC LYMPHADENOPATHY

Although not necessary in typical stage I disease, CT is more sensitive in detecting enlarged lymph nodes than a PA chest x-ray.[54,57] Hilar or mediastinal lymphadenopathy is present on CT in 47 to 94% of patients with sarcoidosis, irrespective of radiographic staging.[41,44,56–60] Lymph nodes are usually bilateral, most commonly with right-sided predominance.[57–60] The distribution of thoracic lymphadenopathy, according to the ATS lymph node map, has been evaluated in two studies.[59,60] The most commonly involved nodal stations, in decreasing order of frequency, were 4R (right lower paratracheal), 10R (right hilar), 7 (subcarinal), 5 (subaortic, i.e., aortopulmonic window), 11R (right interlobar), and 11L (left interlobar).[59,60] The number of enlarged lymph nodes ranged from zero to eight with a median of three, and their maximum short-axis diameter was $\geq$10 mm in 23% of cases and $\geq$20 mm in 16% of cases.[60] Although occasionally present in sarcoidosis, the enlargement of internal mammary and pericardial lymph nodes requires exclusion of lymphoma. Sarcoid lymph nodes are usually nonnecrotic and noncompressive, with calcification frequent in longstanding disease. In a study of patients known to have had disease for up to 32 years, nodal calcification (Fig. 5) was noted in 53%, with eggshell calcification present in 9%.[58] In a further report, calcification was identified at presentation in 20%, increasing to 44% within 4 years.[41]

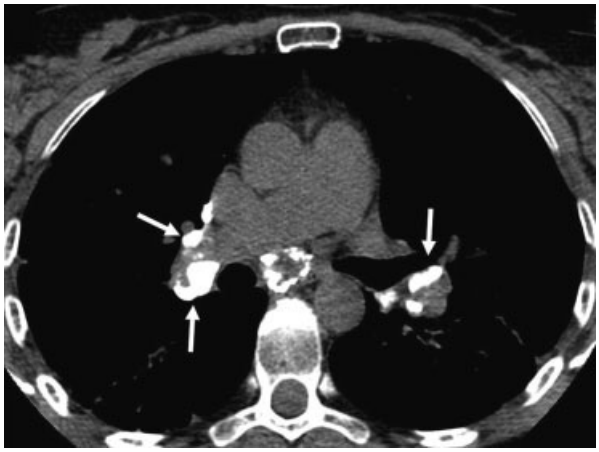

Figure 5 Computed tomographic section showing focal calcification (arrows) of bilateral hilar and subcarinal lymph nodes.

Figure 6 High-resolution computed tomographic section showing widespread nodules more profuse subpleurally on the right.

TYPICAL PARENCHYMAL LESIONS AND PATTERNS

HRCT identifies parenchymal structures lying below the resolution limits of chest radiography but can, nonetheless, be normal in patients with histological proof of lung involvement.[55] The cardinal parenchymal features of sarcoidosis on HRCT are micronodules and nodules, central peribronchovascular thickening, alveolar or pseudoalveolar consolidations, septal and nonseptal lines, ground-glass opacification, signs of lung architectural distortion, conglomerate masses, bronchiectasis, honeycombing or other types of cyst, emphysema, and thickening of the pleural surface.[61,62] CT presentation is influenced by the radiographic stage and disease chronicity. Moreover, multiple CT features or patterns may be variously associated in individual patients and may evolve over time either spontaneously or with therapy.[39–41,44,47,53] Interestingly, in the study of Terasaki et al, CT findings did not differ materially between smokers and nonsmokers, except that emphysema was more extensive in smokers.[52]

Nodular Opacities Nodules are the hallmark of pulmonary sarcoidosis, seen in 80 to 100% of all patients at HRCT[39–42,47,52–56] but less frequently in stage IV.[44] Nodular opacities represent aggregates of granulomas, and CT appearances mirror the histological distribution of sarcoid granulomatous reaction.[63] Nodules have been divided into specific categories according to their size: micronodules < 3 mm; nodules: 3 to 10 mm; irregular marginated nodules: 10 to 20 mm; and alveolar or pseudoalveolar nodules: > 20 mm in diameter.[39,47] Most nodules are small, usually between 1 and 10 mm in diameter, and have irregular poorly circumscribed margins (Fig. 6). Their distribution is widespread but they tend to have a higher profusion around bronchovascular structures and subpleurally, along the concavity of the chest wall, the mediastinum and/or the fissures, along the bronchovascular sheath and the interlobular septa[39,41,55] (Fig. 7). Irregularity or thickening of the bronchovascular bundles is widely cited as a second cardinal sign of pulmonary sarcoidosis.[39,44,47] Peribronchovascular thickening often emanates from the hilar regions in an axial fashion and occasionally gives rise to luminal stenosis.[56] Other diseases distributed along lymphatic channels, such as lymphangitic carcinomatosis and lymphoma, are usually readily distinguished from sarcoidosis on HRCT.[64] Nodularity can result in a fissural or bronchovascular "beaded" aspect, which is widely accepted as virtually pathognomonic of sarcoidosis (although never formally validated).

Small nodules can coalesce into larger nodules over 10 mm in size (Fig. 8), which can very rarely cavitate. Alveolar or pseudoalveolar consolidation consists of large areas of homogeneous intense increased attenuation causing obscuration of bronchovascular margins, with or without an air bronchogram, seen in 12 to 38% of patients.[39,40,42,44,52,53,56] Recently, Nakatsu et al coined the term *sarcoid galaxy* to describe a large nodule, usually with irregular boundaries, encircled by a rim of

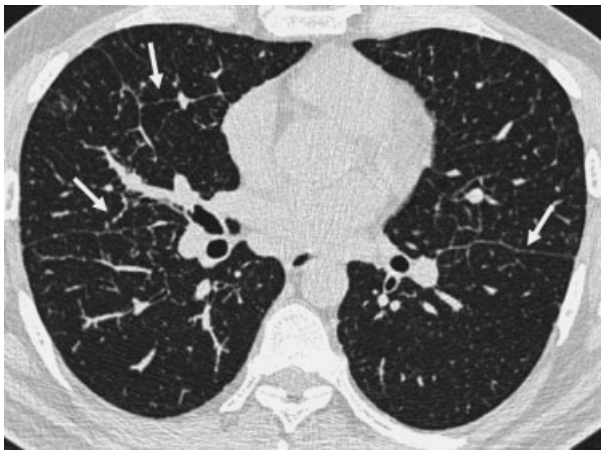

Figure 7 High-resolution computed tomographic section showing micronodules with a typical perilymphatic distribution (i.e., concentrated along the major fissure, the bronchovascular sheaths, and the interlobular septae). There is subtle irregular beading of the fissure and of the polygonal interlobular septae (arrows).

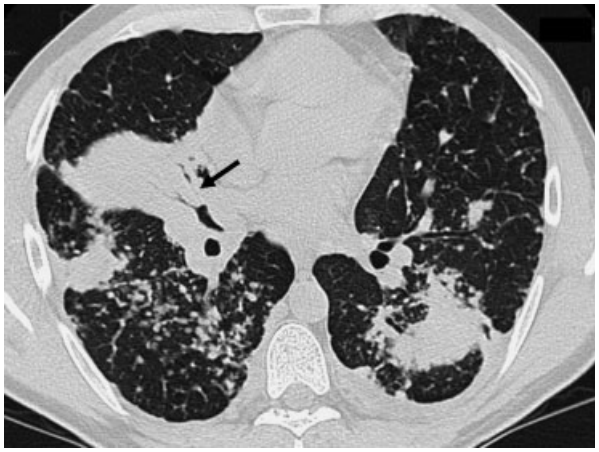

Figure 8 High-resolution computed tomographic section showing poorly defined small nodules with larger nodules and dense consolidation at the lung periphery. There is narrowing of the middle lobe bronchus (arrow) and atelectasis due to right hilar lymphadenopathy. Bilateral pleural thickening is also present.

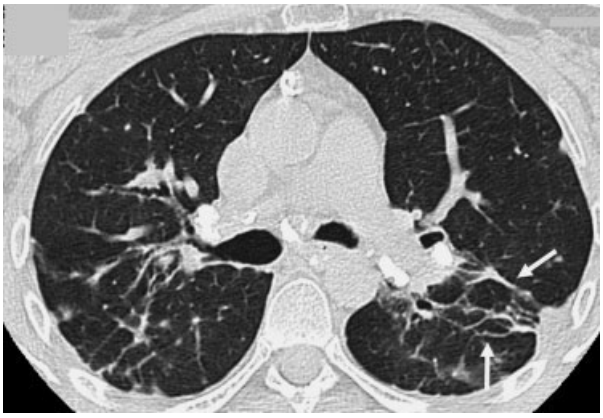

Figure 9 High-resolution computed tomographic section showing a linear pattern, consisting of irregular, mainly hiloperipheral lines (arrows). Multiple calcified lymph nodes are also present.

numerous tiny satellite nodules.[65] In their series of 59 patients with sarcoidosis, 16 (27%) had large nodules, and the "sarcoid galaxy" sign was found in all; sarcoid galaxies were multiple in all but one case, most were 10 to 20 mm in diameter and two contained cavitation. Histologically, a sarcoid galaxy represents innumerable coalescent granulomas that are more concentrated in the center of the lesion.[65] It is likely that sarcoid galaxy lesions overlap with large nodules that were previously named "irregular marginated nodules" or to spherical alveolar or pseudoalveolar consolidation.[62]

Linear Opacities Nodules are the only HRCT abnormality in approximately one third of patients but are more often associated with other patterns.[40,47] Thickened interlobular septae or septal lines are frequent, with a wide reported prevalence range (26 to 89%),[39–42,44,47,53,55] and are usually less profuse than nodules. Nonseptal lines are less frequent and encompass hilar peripheral lines (which are distinct from bronchovascular bundles) (Fig. 9), subpleural lines (which are curvilinear densities paralleling the pleura), and other translobular lines without a precise topography.[39–42,44,47,53,55]Fibrotic lines are often irregular or distorted or both. Linear opacities are sometimes organized as a polygonal configuration in a reticular network, with or without ground-glass[44,47,55] (Fig. 10).

Ground-Glass Opacification Ground-glass opacification is defined as hazy areas of slightly increased attenuation in which vessels and bronchi remain visible. The frequency of ground-glass has a wide reported range (16 to 83%).[39–42,44,47,52,53,56] Ground-glass seems to be more common at presentation than later in the disease course.[47] Although occasionally the predominant abnormality,[47,48,50,51,53,66] ground-glass is usually multifocal rather than diffuse. The histological significance of ground-glass attenuation is varied because granulomatous and fibrotic lesions alike can give rise to this HRCT feature.[63]

Scarring and Fibrosis Lung architectural distortion includes abnormal displacement of hila, fissures, bronchi, or vessels and distortion of secondary pulmonary lobules. Lung architectural distortion is invariable in stage IV disease,[44,47] and, overall, is reported in 20 to 50% of patients.[39–41,47,56] Bronchi may be deformed, angulated, crossed, or stenosed.[44] Bronchial distortion is typically shown by posterior displacement of the main or upper lobe bronchus. This sign, as well as distortion of the major fissure, is likely to indicate loss of lung volume, especially in the posterior segment of the upper lobe.[44] Conglomerate masses are defined as large opacities greater than 3 cm in diameter that often surround and encompass the bronchi and vessels (Fig. 11). Although sometimes difficult to identify, due to amalgamation

Figure 10 High-resolution computed tomographic section showing septal reticulations, ground-glass attenuation, and peribronchovascular thickening, as well as bilateral hilar lymphadenopathy.

Figure 11 High-resolution computed tomographic section showing deformation and angulation of bronchi (arrow); with posterior displacement of the main and upper lobe bronchi (due to segmental volume loss), fibrotic conglomerate masses, and enlargement of the main pulmonary artery.

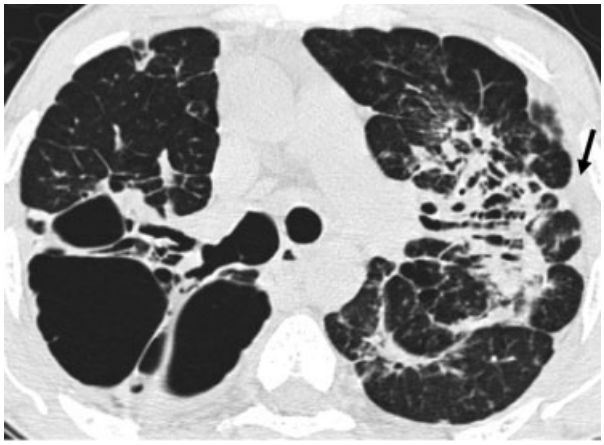

Figure 13 High-resolution computed tomographic section showing a combination of bronchial distortion and linear opacities in the left lung and bullae in the right upper lobe. There is also left pleural thickening (arrow).

with vascular structures, conglomerate masses are a frequent feature in stage IV disease (60%) and are usually central and associated with bronchial distortion.[44] Perihilar conglomerate masses may be indistinguishable from lymphadenopathy.[44]

Traction bronchiectasis, honeycombing, other types of cystic destruction, paracicatricial emphysema, and bullae are relatively rare in sarcoidosis, although more frequent in chronic fibrotic disease. Abehsera et al, in a study of 80 patients with stage IV disease, identified bronchiectasis in 40% and honeycombing in 32% (Fig. 12), with a lower prevalence of cystic abnormalities (19%) and emphysema (12%).[44] Three distinct patterns of distribution were recognized. A bronchial distortion pattern (47%), with or without coexistence masses, was usually central. A honeycombing pattern (29%) was largely peripheral and often occurred predominantly in the upper lobes. A linear pattern (24%) was mainly diffuse.[44] Nodules were less evident in association with a honeycombing pattern, whereas peribronchovascular thickening commonly accompanied bronchial distortion.[44] In the serial HRCT study of Akira et al, ground-glass and consolidation tended to evolve into fibrotic disease, with significant increases in bronchial distortion, honeycombing, traction bronchiectasis, emphysema, and parenchymal bands,[53] in variable combinations (Fig. 13).

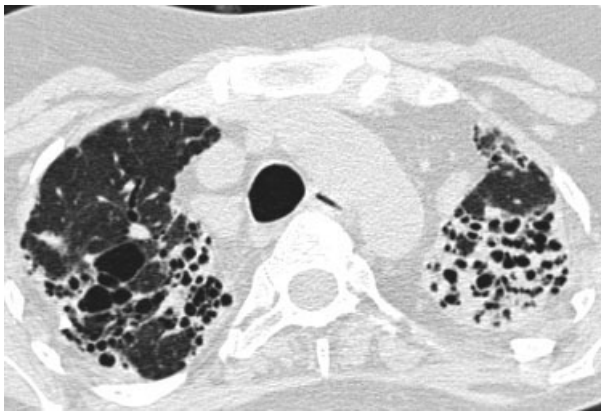

Figure 12 High-resolution computed tomographic section showing honeycomb change.

Airways Involvement Air trapping manifests on HRCT as areas of decreased attenuation, essentially in a mosaic pattern, containing pulmonary vessels of reduced caliber. Air trapping is often obvious on inspiratory images and is enhanced on expiration. Since first reported by Gleeson et al,[67] increasing attention has been devoted to air trapping in sarcoidosis.[48–50,52,68–70] Subsequent studies suggested that expiratory air trapping was common on HRCT, being identified in 83.3 to 98% of patients,[48–50,52,70] and sometimes providing the sole CT evidence of pulmonary sarcoidosis.[50,67] The prevalence and extent of decreased attenuation do not vary according to the chest radiographic stage,[48] the predominant inspiratory CT pattern,[50] or smoking status.[52] It has been suggested that air trapping reflects small-airway obstruction by peribronchiolar or intraluminal granulomas. However, it should be stressed that expiratory air trapping is a nonspecific HRCT sign that is not infrequent in healthy subjects[71]; thus the clinical significance of limited mosaic attenuation is often difficult to interpret.

Bronchomalacia in sarcoidosis has recently been reported in a small series based on volumetric expiratory HRCT images.[70] Lenique et al investigated bronchial appearances on HRCT in 60 patients with sarcoidosis and found that increased bronchial wall thickness and other luminal abnormalities were present in 65% and 23%, respectively, with a positive association between bronchial abnormalities and the presence of mucosal granulomas.[56]

Atypical CT Features

ATYPICAL THORACIC LYMPHADENOPATHY

Lymphadenopathy may be unilateral or localized in an unusual site. Extrinsic compression by enlarged adjacent lymph nodes and/or mediastinal fibrosis is reported in a handful of cases, with compression or distortion of bronchi,[56,72] large pulmonary arteries,[73] the superior vena cava,[74] the esophagus,[75] the left recurrent nerve,[76] or the thoracic duct.[77]

ATYPICAL PARENCHYMAL LESIONS AND PATTERNS

"Nodular" or "Alveolar" Sarcoidosis A predominance of multiple large nodules or an alveolar or pseudoalveolar consolidation ("nodular"[13–15] or "alveolar" sarcoidosis[16] on chest x-ray) can mimic organizing pneumonia or malignancy. The presentation is acute and the prognosis is excellent. Johkoh et al, in a CT evaluation of 10 patients with this appearance, reported homogeneous opacities between 10 and 40 mm in diameter, located along the bronchovascular bundles or subpleurally pleural and characterized by ill-defined contours and many small nodules in the surrounding lung.[78] An air bronchogram was sometimes present, and other CT abnormalities considered typical of sarcoidosis were usually present.

Necrotizing Sarcoid Granulomatosis Necrotizing sarcoid granulomatosis (NSG) is characterized histologically by a sarcoid-like granulomatous reaction with vasculitis (involving both arteries and veins) and noncaseating necrosis.[79] NSG and "nodular"/"alveolar" sarcoidosis share many clinical and radiological features but appear to be separate entities, nonetheless. In a recent study of 14 patients with NSG, the most common CT feature was alveolar opacities, seen in seven cases (50%), and these were mainly subpleural without predilection for any single lobar site; other variable findings included a bronchogram, a solitary nodule, bilateral/multiple nodules, cavitation, bilateral hilar or mediastinal adenopathy, and pleural thickening.[80]

Cavitation Cavitation is more easily diagnosed on CT than on chest radiograph and must be distinguished from cystic bronchiectasis and bullous change (Fig. 14).[47,54] Because primary cavitary sarcoidosis is rare, superimposed infection, and Wegener's granulomatosis should always be excluded. The development of sarcoid cavities is believed to result from either ischemic necrosis (with extrusion of hyaline material from conglomerate sarcoid granulomas) or vasculitis. The frequency of cavitation in a chest radiographic study was 0.8%,[4] and in two CT studies, cavitation of nodules was seen in three of 44 patients (6.8%) and in two of 59 patients (3.4%), respectively.[47,65] Based on a handful of case reports,[81–85] cavitation usually develops inside nodules or alveolar condensation and may be seen on CT following presentation with a pneumothorax.[83,85] In our experience, cavitary lesions are usually small, thin walled, and, although occasionally found in isolation, more likely to be multiple and bilateral, although seldom present in large numbers.

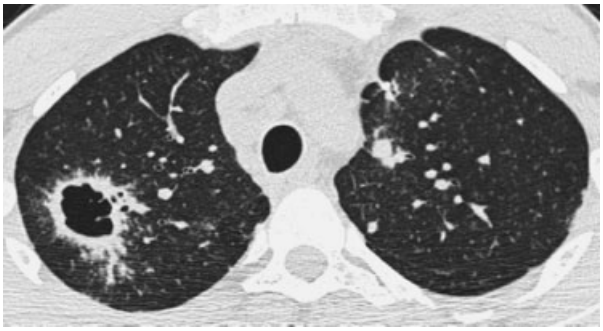

Figure 14 High-resolution computed tomographic section showing cavitation in a large nodule with multiple confluent small nodules in the surrounding lung. This appearance required the exclusion of bacterial infection, aspergilloma, tuberculosis or nontuberculous mycobacterial infection, and Wegener's granulomatosis.

Sarcoidosis Mimicking Idiopathic Pulmonary Fibrosis The typical CT appearances of fibrotic sarcoidosis and idiopathic pulmonary fibrosis (IPF) are very dissimilar. Honeycombing is rare in sarcoidosis and, when present, usually affects the upper and perihilar regions.[44] Interestingly, in a few cases of histologically confirmed sarcoidosis, honeycombing had a striking prominence in the lower lung zones with a peripheral and subpleural distribution, or was diffuse. This pattern has been reported in a total of six patients.[44,86]

Other Atypical Parenchymal Lesions and Patterns Nodules may be sparse in distribution rather than widespread. They may be dispersed throughout lungs without any topographic predilection[47] or may very rarely have a hematogenous or centrilobular distribution (rather than a perilymphatic distribution), mimicking miliary tuberculosis and hypersensitivity pneumonitis, respectively.[87] Masslike solitary nodules and alveolar consolidation at a single focus are exceedingly rare in sarcoidosis.[88–90] One patient presented with diffuse ground-glass attenuation on CT, which oddly shifted to the peripheral lung zones and later developed both micronodular lesions and enlarged thoracic lymph nodes.[91] A "halo sign,"[92] a "fairy ring" sign,[93] and profuse micronodular calcification have also been described.[94]

PLEURAL INVOLVEMENT

Pleural involvement is better detected on CT than on chest x-ray.[95] Pleural effusions may result from pleural granulomatous involvement or from the blockage of

interlobular septal lymphatic channels by granulomas. Apparent pleural thickening often represents inward retraction of extrathoracic soft tissue and extrapleural fat, rather than a true pleural abnormality.[62] Pleural involvement is rare in sarcoidosis, with pleural effusions observed in less than 5% on chest radiography.[10,11] In CT studies, pleural thickening surface is present in 11 to 27% of patients.[41,47,54,56] However, in the recent study of Szwarcberg et al the frequency of pleural involvement reached 41%, including thickening in 32.8% of cases, mainly associated with pulmonary fibrosis, and a limited effusion in 8.2% of cases.[95]

Diagnostic Role of CT

The diagnostic superiority of CT over chest radiography in DLD has been clearly demonstrated.[31–36] When studied populations were grouped, the overall diagnostic sensitivity of CT for pulmonary sarcoidosis was 78% as opposed to 70% for chest radiography.[61,62] Grenier et al evaluated supplementary information yielded by CT after taking into account clinical data and radiographic findings.[35] Computer-aided diagnoses were made by applying a Bayesian model in a large population of 308 patients with DLDs, including 121 with pulmonary sarcoidosis. For sarcoidosis, the overall sensitivity (utilizing two observers) was 76 to 83% with clinical data alone, 80 to 88% with clinical and radiographic findings, and 85 to 90% with the addition of CT. The percentages of correct diagnosis with a high level of confidence were respectively 33 to 42%, 52 to 76%, and 78 to 80%.[35] This relatively small difference emphasizes the fact that CT adds little when clinical and radiographic presentation is typical of sarcoidosis, understates the true diagnostic value of CT in other, less straightforward cases.

In atypical variants, CT often increases the diagnostic likelihood of sarcoidosis, especially when unusual features are associated with more characteristic patterns: atypical CT features seen in isolation makes the disease difficult to diagnose.

Thoracic lymphadenopathy on CT is usual in sarcoidosis but is not a specific CT feature. Niimi et al found that lymphadenopathy was also common in collagen vascular disease (70%), IPF (67%), extrinsic allergic alveolitis (53%), and organizing pneumonia (36%). However, the number of enlarged nodes was higher in sarcoidosis than in other DLDs (mean 3.2 vs 1.2), and all patients with nodes $\geq$ 20 mm in short-axis diameter had sarcoidosis.[60]

Conversely, the pattern and distribution of lymph node calcification may be an important ancillary diagnostic sign on CT to distinguish between sarcoidosis and an alternative DLD associated with. a previous episode of tuberculosis. Gawne-Caine and Hansell showed that the mean diameter of calcified nodes was significantly larger in sarcoidosis (12 mm vs 7 mm); calcium deposition was more commonly focal in sarcoidosis (58% vs 23%) and diffuse in tuberculosis (27% vs 62%), and, when present, hilar nodal calcification was more likely to be bilateral in sarcoidosis than in tuberculosis (65% vs 8%).[58]

CT FOR NORMAL CHEST RADIOGRAPH BUT CLINICAL SUSPICION OF SARCOIDOSIS

Ascertaining the diagnosis of sarcoidosis is sometimes problematic when sarcoidosis is confined to one organ. CT may facilitate the diagnosis when standard diagnostic tests are negative or equivocal (as is commonly the case in uveitis) or when a biopsy of an extrapulmonic site is considered too risky (as in central nervous system involvement). In one study of uveitis, CT was especially useful in elderly women with normal chest radiographic appearances.[96]

CT AND THE DETECTION OF COMPLICATIONS

The value of CT in the detection of complications has never been formally quantified but is amply validated by clinical experience, especially when there is unexplained worsening of respiratory symptoms, hemoptysis, disproportionate impairment of PFTs or airflow obstruction, uncertain chest radiographic abnormalities, aspergilloma, or PH.[1,97]

Aspergilloma Mycetoma formation is a frequent complication of stage IV disease, particularly in patients with advanced fibrocystic or cavitary disease.[5,98] Aspergilloma is more readily visualized using CT, which generally reveals a cavity containing a well-defined homogeneous nodule, with or without a characteristic air crescent (Fig. 15).[99] Fungus balls can be mobile, as judged by movement within a cavity with a change from the supine to the prone position. Aspergillomas are often associated with thickening of the cavity wall and adjacent pleura, which is sometimes the earliest sign before any visible

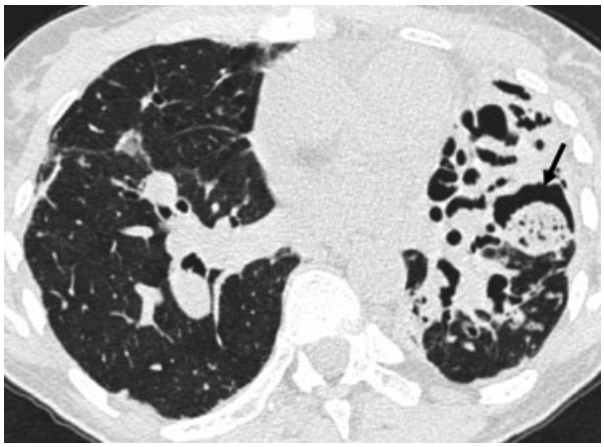

Figure 15 High-resolution computed tomographic section showing an aspergilloma (arrow) in a cavity with a characteristic air crescent.

changes are seen within the cavity.[99] Aspergilloma may be multiple and bilateral, and this is best appreciated by CT and imperative to recognize before surgery.

Pulmonary Hypertension PH is not uncommon in advanced disease[100] and is usually attributed to the destruction of the distal capillary bed by fibrotic process or to chronic hypoxemia or both. However, it has also been reported in the early stages of the disease with marginal or no pulmonary involvement,[73] suggesting alternative pathogenetic mechanisms, including extrinsic compression of large pulmonary arteries (Figs. 16 and 17) by enlarged lymph nodes or mediastinal fibrosis[101,102]; specific granulomatous vascular involvement,[101,103] which sometimes simulates secondary pulmonary veno-occlusive disease[104]; and pulmonary vasoconstriction by vasoactive factors.[105] Contrast-enhanced CT may raise the possibility of PH when the main pulmonary artery is larger than 30 mm in diameter and may also help to identify underlying mechanisms,[73] but pulmonary angiography is often required to confirm compression by extravascular structures.[73]

Bronchial Stenosis Symptomatic bronchial stenosis is rare and may develop at any stage of the disease.[56,72] Obstruction may be the consequence of endobronchial granulomatous involvement, external compression by enlarged lymph nodes, or severe architectural distortion. For anatomical reasons, the right middle lobe is most often affected.[72] Apart from showing atelectasis, CT is sometimes useful in determining the extent and nature of bronchial stenosis.[56]

Prognostic Role of CT

Correlations between CT findings and classic markers of sarcoidosis activity, including serum angiotensin-converting enzyme (ACE) levels, bronchoalveolar lavage findings, and gallium scan signal, have been inconclusive or discrepant.[31,38,40,42,43,47] Much more has been learned from studies of the reversibility of CT features (with or without treatment) on serial scanning.[39–41,53] Architectural distortion, traction bronchiectasis, honeycombing, and bullae are consistently irreversible. Micronodules, nodules, peribronchovascular thickening, and consolidation are wholly or partially reversible in most (but not all) cases. The evolution of ground-glass attenuation and linear opacities is more variable. Ground-glass opacities may steady, worsen, or improve over time, with or without treatment,[39–41,53] reflecting the fact that ground glass may represent either granulomas or fine fibrosis.[63,66] As in other DLDs, a coarse texture or concomitant traction bronchiectasis increases the likelihood of underlying fibrosis.[66] Similarly, septal thickening from intense granulomatous infiltration is likely to reverse, but other linear opacities are more likely to be fibrotic.

Discrimination between active inflammation and irreversible fibrosis with CT is appealing in theory but seldom employed in practice, perhaps because decisions on the need for treatment are straightforward in most cases. However, CT may occasionally be helpful when the decision to initiate or continue potentially toxic treatment is marginal. For instance, in stage IV disease a trial of therapy might be warranted if a potentially reversible component is visible on CT.[44]

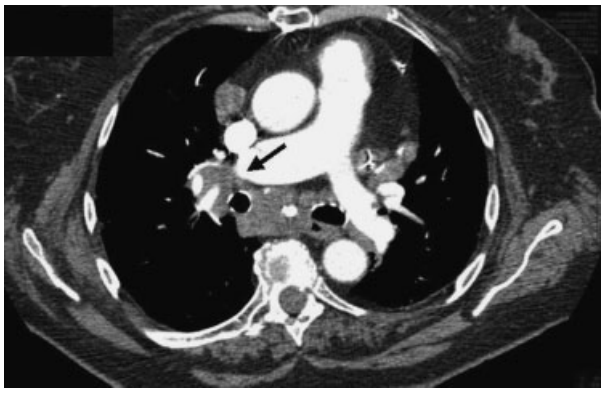

Figure 16 Enhanced computed tomographic section from a patient with moderate pulmonary hypertension showing extrinsic compression of the main right artery by lymphadenopathy (arrow). There is prestenotic enlargement of the right pulmonary artery.

Figure 17 Pulmonary angiogram from a patient with moderate pulmonary hypertension confirming the presence of concentric stenosis of the intermediary pulmonary artery consistent with extrinsic compression (arrow).

CORRELATIONS BETWEEN CT AND PULMONARY FUNCTION TESTS

Correlations between CT findings and PFTs have been examined in many studies[40,44–53] with variable results,

probably reflecting the diversity of CT scoring systems. In most reports, the degree of functional impairment, as assessed by gas transfer levels and spirometric volumes, is usually linked to an overall CT score,[40,44–53] but most correlations are weak[45–47,51] and CT is not consistently superior to chest radiography.[45–47,51] Hansell demonstrated that the extent of reticular abnormalities was strongly and independently associated with several indices of airflow obstruction.[29] Abehsera et al. showed that in stage IV disease, bronchial distortion was associated with lower expiratory airflow rates, honeycombing was associated with restriction and lower diffusing capacity for carbon monoxide (DL_{CO}), but functional impairment was relatively minor when nondestructive linear abnormalities predominated.[44] Air trapping is associated with evidence of small-airway obstruction, including maximal midrespiratory flow rates at 25 to 75% of the vital capacity (MMEF25–75), residual volume (RV), and/or RV/total lung capacity (TLC),[48–50] although this was not the case in one report.[52]

OTHER IMAGING TECHNIQUES

Magnetic resonance imaging (MRI) is seldom useful in evaluation of the lung parenchyma because of imaging limitations, due mainly to the composition of lung tissue and physiological motion (cardiac pulsation and respiration). Despite these inherent pitfalls, several authors have studied thoracic MRI in sarcoidosis[106,107] or DLD at large.[108–111] All studies but one used unenhanced T1- and T2-weighted MRI[106–110] with unconvincing results,[112] and MRI was inferior to HRCT.[109] More recently Gaeta et al first used gadolinium-enhanced thoracic MRI in a DLD cohort including 10 patients with sarcoidosis[111] and showed enhancement of pulmonary lesions in five of seven patients with active disease. However, it appears highly unlikely that MRI will supplant HRCT in the foreseeable future.

The lung clearance of inhaled technetium-99m labeled diethylene triamine penta-acetic acid (^{99m}Tc-DTPA) has been studied in pulmonary sarcoidosis.[113–120] An increased rate of lung clearance has been associated with disease activity in some studies[113,114] but not in others,[115,118] and with functional deterioration.[116] DTPA clearance sometimes returns to normal with corticosteroid therapy.[116,118] However, the role of this test in the management of sarcoid patients remains largely speculative.

CENTRAL NERVOUS SYSTEM SARCOIDOSIS

Central nervous system (CNS) involvement occurs in less than 10% of patients with sarcoidosis.[1,5,120] Although any part of the CNS can be affected, sarcoidosis has a strong predilection for the base of the skull, hypothalamus, pituitary gland, and optic chiasma.[112,121] The development of neurosarcoidosis is primarily leptomeningeal and vascular (Fig. 18) in nature. It may follow disruption of the leptomeningeal blood–brain barrier, permitting the spread of the granulomatous process to the brain parenchyma along the so-called perivascular or Virchow-Robin spaces that accompany the penetrating arteries up to the capillaries.[112,121] As a consequence, two types of lesion are observed: coalescent intraparenchymal granulomas and small ischemic foci.[107,108] Imaging is pivotal for the diagnosis of CNS sarcoidosis, especially in patients without systemic evidence of disease, because CNS biopsy is seldom justifiable.

MRI

Contrast-enhanced brain CT is insensitive, with normal appearances in up to a third of patients with definite CNS sarcoidosis, especially when lesions are confined to the cranial or peripheral nerves or brainstem.[62] CNS sarcoidosis may still be imperceptible at MRI in some patients with cranial nerve or neuroendocrine symptoms[122] but is clearly more sensitive than CT.[112,121,123] Thus gadolinium-enhanced MRI is the diagnostic investigation of choice in suspected CNS sarcoidosis.

Leptomeningeal involvement, the most frequent feature, may not be apparent with nonenhanced MRI.[124,125] It typically manifests as thickening and enhancement of leptomeninges on T1-weighted images, usually at the base of the skull. The abnormal signal may be diffuse or nodular[112,121] and is indistinguishable from abnormalities seen in tuberculosis or malignancy.[112,121] Focal dural masses may also mimic meningioma.[112,121] *Intraparenchymal involvement* is usually evident on MRI as multifocal periventricular, subcortical, or deep white matter lesions (Fig. 19).[112,121] These

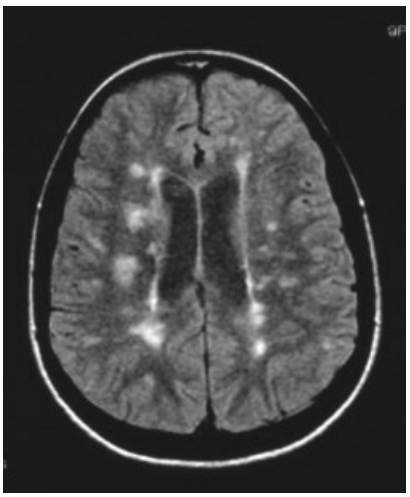

Figure 18 Axial contrast-enhanced T1-weighted brain magnetic resonance image showing a typical multifocal enhancement after gadolinium in the periventricular zone and along the penetrating arteries.

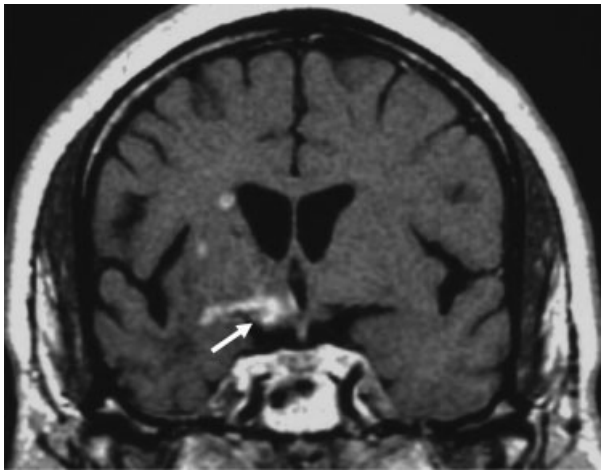

Figure 19 Coronal proton density-weighted brain magnetic resonance image demonstrating hyperintense deep white matter lesions that did not enhance after gadolinium and infiltrative lesions in the chiasmatic area (arrow).

abnormalities are nonspecific and may be identical to those seen in vascular disease or multiple sclerosis.[112,121] Multiple or solitary space-occupying lesions, usually without central necrosis, are not infrequent and may simulate malignancy due to extensive surrounding edema.[112,121] Intraparenchymal lesions are frequently clustered near regions of leptomeningeal involvement. Recent and active inflammatory lesions usually enhance after gadolinium injection on T1-weighted images, whereas irreversible lesions do not enhance and typically display hyperintense signal on T2-weighted images.[122,126,127] *Hypothalamus and pituitary infiltration* (Fig. 20) ranges from a thickening of pituitary infundibulum, indistinguishable from findings in Langerhans' cell hystiocytosis, to an intra- or suprasellar mass.[112,121] *Intramedullary lesions* manifest as a fusiform enlargement of the spinal cord in the cervical or upper thoracic level (Fig. 21), appearing in weighted images and after gadolinium injection, depending upon the stage of disease stage.[112,121,128] Neurological complications, such as an obstructive or communicating hydrocephalus, may also be disclosed by MRI.[121] Despite the high frequency of histological vasculitis in CNS sarcoidosis, large brain infarcts are rare.[121]

Unfortunately, MRI manifestations are not pathognomonic of sarcoidosis.[127,129] However, the enhancement of intraparenchymal lesions and the coexistence of leptomeningeal enhancement are highly suggestive in an appropriate clinical context.[112] MRI may also have a prognostic role: lesions enhancing with gadolinium are more likely to regress with therapy.[122,126,127] Sequential MRI is sometimes useful in monitoring patients with CNS sarcoidosis,[126,127] but symptomatic improvement often correlates poorly with MRI change,[122] especially in spinal cord disease.[130]

CARDIAC SARCOIDOSIS

Clinical evidence of cardiac involvement is present in ~5% of sarcoidosis patients,[1,5,131] although cardiac abnormalities are more prevalent in Japan.[1,131] Histologically, the myocardium is most frequently involved, but granulomas may also be found in the pericardium, myocardium, and endocardium. The predominant sites of myocardial involvement, in decreasing order of frequency, are left ventricular free wall and papillary

Figure 20 Midsagittal contrast-enhanced T1-weighted brain magnetic resonance image demonstrating a gadolinium-enhancing mass of the floor of the third ventricle and hypothalamus (arrow).

Figure 21 Sagittal T1-weighted magnetic resonance image of the spinal cord showing an intramedullary gadolinium-enhancing mass responsible for cordal enlargement (arrow).

muscles, the intraventricular septum, the right ventricular wall, the right atrium, and the left atrium.[131] The diagnostic evaluation of cardiac involvement is undeniably one of the most challenging management issues in sarcoidosis. No diagnostic reference standard exists because endomyocardial biopsy is invasive and lacks sensitivity as a result of sampling error. Official guidelines from the Japanese Ministry of Health and Welfare include the results of histological analysis, electrocardiogram (ECG), echocardiography, thallium-201 (^{201}Tl) or technetium-99m (^{99m}Tc) myocardial scintigraphy or gallium-67-citrate (^{67}Ga) scan, and cardiac catheterization.[131] However, these guidelines have never been prospectively validated and they predate the advent of newer techniques such as ^{67}Ga plus ^{99m}Tc-MIBI[132] and single-photon emission computed tomography.[132,133] Moreover, there is emerging evidence that cardiac MRI (CMR)[112,131,134–141] and fluorine 18 fluorodeoxyglucose (^{18}FDG) positron emission tomography (PET)[142–144] may be clinically useful.

Cardiac MRI

CMR has a unique ability to provide detailed anatomical information and, also, to quantify global and regional ventricular function by means of cine sequences.[112,131,134] CMR typically shows zones of thinning and segmental myocardial wall motion abnormalities with increased signal intensity (Fig. 22), more pronounced on T2-weighted images because of associated edema, and variably enhancing with gadolinium.[112,131,134] The pattern of enhancement follows the histological distribution of granulomas and differs from that seen in ischemic disease.[112,131,134] The sensitivity and specificity of CMR remain uncertain. Smedema et al evaluated the accuracy of CMR in a series of 58 patients with suspected cardiac sarcoidosis, using the Japanese guidelines[131] as a "gold-standard," and found a sensitivity and specificity of 100% and 78%, respectively.[139] In a further study, Smedema et al compared CMR with standard assessment in 55 patients with pulmonary sarcoidosis who were investigated because of cardiac symptoms or for screening purposes.[141] CMR was abnormal in all 13 patients diagnosed with cardiac sarcoidosis by the standard assessment and detected six additional patients in whom ECG, ambulatory ECG, Doppler-echocardiography, and ^{201}Tl scintigraphy were wholly normal. Thus CMR may detect early cardiac involvement when a conventional approach fails to do so.[137] However, the clinical relevance of limited CMR abnormalities was difficult to quantify as patient follow-up, though short, was uneventful.[141] The extent of enhancement correlated with disease severity, especially ventricular dilatation, functional impairment (Fig. 23) and the presence of ventricular arrhythmias.[141]

Serial studies show that enhanced areas markedly regress or normalize completely with corticosteroid therapy[135,137] in parallel with clinical improvement.[137] The major drawback of CMR is that it cannot be used in patients with cardiac implantable devices, which are frequently required in cardiac sarcoidosis.[112,131] Further systematic multicenter studies are required to construct a clinically useful diagnostic algorithm for CMR in the detection and management of cardiac sarcoidosis.

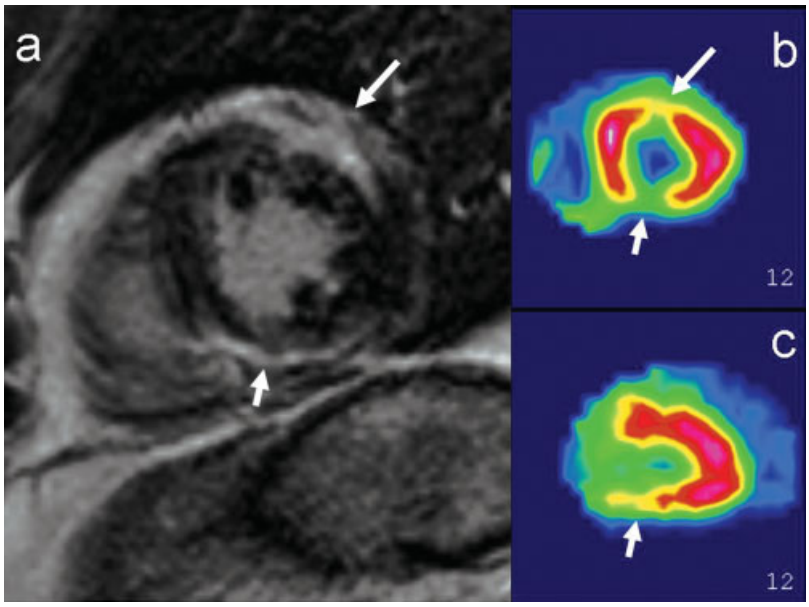

Figure 22 Delayed enhanced cardiac magnetic resonance imaging [short axis view (a)] demonstrating a transmural late enhancement of the anterolateral area (long arrow) and a subepicardial late enhancement of the inferoseptal area (short arrow). Single photon emission computed tomography [short axis (b) and vertical long axis (c) views] demonstrates perfusion abnormalities in the same areas.

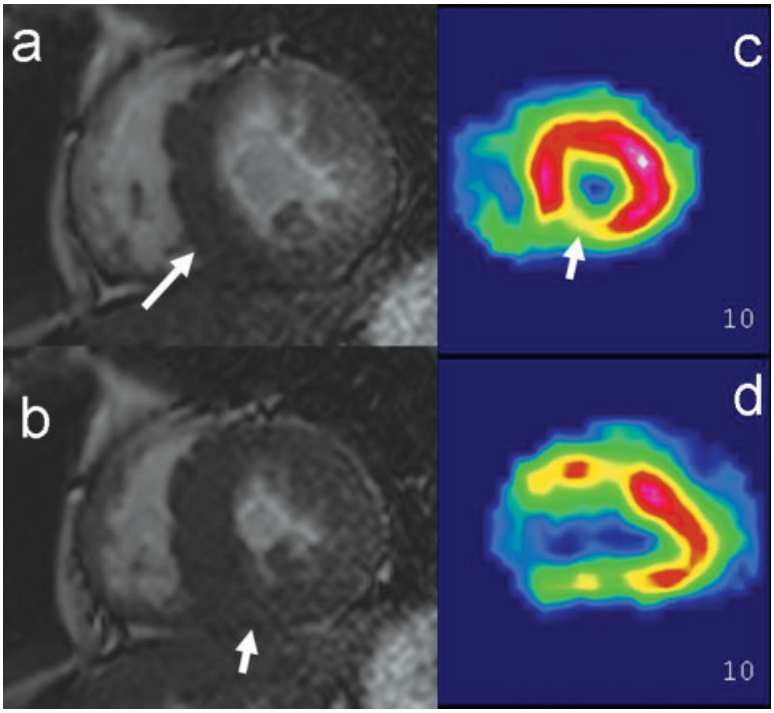

Figure 23 Three-dimensional breath-hold cardiac magnetic resonance (short axis) in diastole (a) and systole (b) demonstrating septal thickening and functional impairment in the inferoseptal area (arrows) with corresponding perfusion abnormalities at single photon emission computed tomography [short axis (c) and vertical long axis (d) views].

^{18}FDG PET

^{18}FDG PET has been compared with ^{67}Ga,[142–144] ^{201}Tl,[142] and ^{99m}Tc-MIBI scintigraphy[143,144] in patients with cardiac sarcoidosis according to the Japanese guidelines. The sensitivity of ^{18}FDG PET was 100%, which was higher than that of the other methods.[128,129] By contrast, its specificity was slightly lower at 81.5 to 90.9%. Yamagishi et al showed that ^{18}FDG uptakes either diminished in size and density or disappeared under corticosteroids.[142] Further studies are still needed before any definite statement can be made on the exact role of ^{18}FDG PET.

Other Imaging Techniques

Other imaging techniques have been tested in cardiac sarcoidosis but data are sporadic: myocardial scintigraphy with the use of iodine-123-labeled 15-(p-iodophenyl)-3R,S-methylpentadecanoic acid,[145] a creative technique of ultrasonic tissue characterization, which noninvasively measures acoustic properties of the myocardium,[146] and contrast-enhanced mutlislice CT.[147]

SPECIFIC IMAGING TECHNIQUES

^{67}Ga Scanning

The sensibility of ^{67}Ga scan in detecting pulmonary sarcoidosis ranges from 60 to 90%.[112] The characteristic appearances of ^{67}Ga uptake in sarcoidosis has been referred to as the "lambda" and "panda" patterns.[112,148] The lambda pattern consists of bilateral symmetrical uptake in the parahilar and infrahilar lymph nodes, together with right paratracheal lymph node uptake, and may be observed even when the chest radiograph is normal. Symmetrical uptake in the parotid, lacrimal, and salivary glands with normal nasopharyngeal capture produces a picture similar to the face of a panda.[112,148] The "lambda plus panda" pattern, and the panda pattern coupled with bilateral hilar lymphadenopathy or bilateral parenchymal infiltration on chest radiography, are believed to be highly specific for sarcoidosis. However, a panda pattern in isolation lacks specificity, occurring as in other clinical contexts including lymphoma.[112,148–150] It has been argued that the presence of the lambda plus panda pattern may obviate a tissue diagnosis.[1]

Uptake of ^{67}Ga is seen in a variety of extrapulmonary sites,[151] in addition to normal uptake in the liver and spleen, but the low sensitivity and specificity of abnormal uptake limits the value of ^{67}Ga scintigraphy in the evaluation of specific organ involvement. The usefulness of ^{67}Ga scan as an index of activity has been examined in several studies,[152–157] but despite correlations with serum ACE levels[154–156] and bronchoalveolar lavage findings,[152,153,157] the results have been inconclusive or conflicting.[112] Similarly, ^{67}Ga scan is not believed to be useful in prognostic evaluation or monitoring.[112]

^{18}FDG PET

Recently, several reports on ^{18}FDG PET in sarcoidosis have appeared. ^{18}FDG is taken up in several sites in sarcoidosis but the sensitivity and specificity of abnormal signal is uncertain. ^{18}FDG may be most useful in diagnosing cardiac sarcoidosis.[142–144] Brudin et al compared regional pulmonary ^{18}FDG metabolism with PFTs, chest radiography, and serum ACE (SACE) levels, initially and after corticosteroid therapy, in seven patients with sarcoidosis.[158] The degree of ^{18}FDG uptake correlated well with SACE levels and disease extent at different stages and normalized during treatment.[158] Yamada et al evaluated the uptake of ^{18}FDG and carbon-11 labeled methionine in 31 patients with intrathoracic sarcoidosis lymphadenopathy. By using the ratio of ^{18}FDG to methionine in pretreatment evaluation, they were able to predict posttherapy improvement as assessed clinically and by chest radiography. In the ^{18}FDG dominant group (ratio ≥ 2), the response rate was 78% but in the methionine dominant group (ratio < 2) it dropped to 38%.[159] Enthusiasm for ^{18}FDG PET should be tempered by concerns over its radiation dose and cost.

REFERENCES

1. Statement on sarcoidosis. Joint Statement of the American Thoracic Society (ATS), the European Respiratory Society (ERS) and the World Association of Sarcoidosis and Other Granulomatous Disorders (WASOG) adopted by the ATS Board of Directors and by the ERS Executive Committee, February 1999. Am J Respir Crit Care Med 1999;160:736–755
2. Nunes H, Soler P, Valeyre D. Pulmonary sarcoidosis. Allergy 2005;60:565–582
3. Lynch JP, Kazerooni EA, Gay SE. Pulmonary sarcoidosis. Clin Chest Med 1997;18:755–785
4. Mayock RL, Bertrand P, Morrison CE, Scott JH. Manifestations of sarcoidosis. Analysis of 145 patients, with a review of nine series selected from the literature. Am J Med 1963;35:67–89
5. Johns CJ, Michele TM. The clinical management of sarcoidosis: a 50-year experience at the John Hopkins Hospital. Medicine (Baltimore) 1999;78:65–111
6. Scadding JG. Prognosis of intrathoracic sarcoidosis in England. Br Med J 1961;2:1165–1172
7. Mana J, Gomez-Vaquero C, Montero A, et al. Lofgren's syndrome revisited: a study of 186 patients. Am J Med 1999;107:240–245
8. Winterbauer RH, Belic N, Moores KD. Clinical interpretation of bilateral hilar adenopathy. Ann Intern Med 1973; 78:65–71
9. Bein ME, Putman CE, McLoud TC, Mink JH. A reevaluation of intrathoracic lymphadenopathy in sarcoidosis. AJR Am J Roentgenol 1978;131:409–413
10. Littner MR, Schachter EN, Putman CE, et al. The clinical assessment of roentgenographically atypical pulmonary sarcoidosis. Am J Med 1977;62:361–368
11. Rockoff SD, Rohatgi PK. Unusual manifestations of thoracic sarcoidosis. AJR Am J Roentgenol 1985;144:513–528
12. Conant EF, Glickstein MF, Mahar P, et al. Pulmonary sarcoidosis in the older patient: conventional radiographic features. Radiology 1988;169:315–319
13. Sharma OP, Hewlett R, Gordonson J. Nodular sarcoidosis: an unusual radiographic appearance. Chest 1973;64:189–192
14. Onal E, Lopata M, Lourenco RV. Nodular pulmonary sarcoidosis: clinical, roentgenographic, and physiologic course in five patients. Chest 1977;72:296–300
15. Romer FK. Sarcoidosis with large nodular lesions simulating pulmonary metastases: an analysis of 126 cases of intrathoracic sarcoidosis. Scand J Respir Dis 1977;58:11–16
16. Battesti JP, Saumon G, Valeyre D, et al. Pulmonary sarcoidosis with an alveolar radiographic pattern. Thorax 1982;37:448–452
17. Tazi A, Desfemmes-Baleyte T, Soler P, et al. Pulmonary sarcoidosis with a diffuse ground-glass pattern on the chest radiograph. Thorax 1994;49:793–797
18. Rohatgi PK, Schwab LE. Primary acute pulmonary cavitation in sarcoidosis. AJR Am J Roentgenol 1980;134: 1199–1203
19. Sharma OP, Gordonson J. Pleural effusion in sarcoidosis: a report of six cases. Thorax 1975;30:95–101
20. Soskel N, Sharma OP. Pleural involvement in sarcoidosis: case presentation and detailed review of the literature. Semin Respir Med 1992;13:492–514
21. Mendelson DS, Norton K, Cohen BA, et al. Bronchial compression: an unusual manifestation of sarcoidosis. J Comput Assist Tomogr 1983;7:892–894
22. Munt PW. Middle lobe atelectasis in sarcoidosis. Am Rev Respir Dis 1973;108:357–360
23. Siltzbach LE, James DG, Neville E, et al. Course and prognosis of sarcoidosis around the world. Am J Med 1974; 57:847–852
24. Romer FK. Presentation of sarcoidosis and outcome of pulmonary changes. Dan Med Bull 1982;29:27–32
25. Hillerdal G, Nou E, Osterman K, et al. Sarcoidosis: epidemiology and prognosis: a 15-year European study. Am Rev Respir Dis 1984;130:29–32
26. Gibson GJ, Prescott RJ, Muers MF, et al. British Thoracic Society Sarcoidosis study: effects of long term corticosteroid treatment. Thorax 1996;51:238–247
27. Pietinalho A, Tukiainen P, Haahtela T, et al. Oral prednisolone followed by inhaled budesonide in newly diagnosed pulmonary sarcoidosis: a double-blind, placebo-controlled multicenter study. Finnish Pulmonary Sarcoidosis Study Group. Chest 1999;116:424–431
28. Pietinalho A, Tukiainen P, Haahtela T, et al. Early treatment of stage II sarcoidosis improves 5-year pulmonary function. Chest 2002;121:24–31
29. Hansell DM. High-resolution CT of diffuse lung disease: value and limitations. Radiol Clin North Am 2001;39: 1091–1113
30. Beigelman-Aubry C, Hill C, Guibal A, Savatovsky J, Grenier PA. Multi-detector row CT and postprocessing techniques in the assessment of diffuse lung disease. Radiographics 2005;25:1639–1652
31. Bergin CJ, Coblentz CL, Chiles C, et al. Chronic lung diseases: specific diagnosis by using CT. AJR Am J Roentgenol 1989;152:1183–1188

32. Mathieson JR, Mayo JR, Staples CA, et al. Chronic diffuse infiltrative lung disease: comparison of diagnostic accuracy of CT and chest radiography. Radiology 1989;171:111–116
33. Padley SP, Hansell DM, Flower CD, et al. Comparative accuracy of high-resolution computed tomography and chest radiography in the diagnosis of chronic diffuse infiltrative lung disease. Clin Radiol 1991;44:222–226
34. Grenier P, Valeyre D, Cluzel P, et al. Chronic diffuse interstitial lung disease: diagnostic value of chest radiography and high-resolution CT. Radiology 1991;179:123–132
35. Grenier P, Chevret S, Beigelman C, et al. Chronic diffuse infiltrative lung disease: determination of the diagnostic value of clinical data, chest radiography, and CT and Bayesian analysis. Radiology 1994;191:383–390
36. Nishimura K, Izumi T, Kitaichi M, et al. The diagnostic accuracy of high-resolution computed tomography in diffuse infiltrative lung diseases. Chest 1993;104:1149–1155
37. Mana J, Teirstein AS, Mendelson DS, et al. Excessive thoracic computed tomographic scanning in sarcoidosis. Thorax 1995;50:1264–1266
38. Lynch DA, Webb WR, Gamsu G, et al. Computed tomography in pulmonary sarcoidosis. J Comput Assist Tomogr 1989;13:405–410
39. Brauner MW, Lenoir S, Grenier P, et al. Pulmonary sarcoidosis: CT assessment of lesion reversibility. Radiology 1992;182:349–354
40. Remy-Jardin M, Giraud F, Remy J, et al. Pulmonary sarcoidosis: role of CT in the evaluation of disease activity and functional impairment and in prognosis assessment. Radiology 1994;191:675–680
41. Murdoch J, Müller NL. Pulmonary sarcoidosis: changes on follow-up CT examination. AJR Am J Roentgenol 1992; 159:473–477
42. Leung AN, Brauner MW, Caillat-Vigneron N, et al. Sarcoidosis activity: correlation of HRCT findings with those of 67Ga scanning, bronchoalveolar lavage, and serum angiotensin-converting enzyme assay. J Comput Assist Tomogr 1998;22:229–234
43. Oberstein A, von Zitzewitz H, Schweden F, Muller-Quernheim J. Noninvasive evaluation of the inflammatory activity in sarcoidosis with high-resolution computed tomography. Sarcoidosis Vasc Diffuse Lung Dis 1997;14: 65–72
44. Abehsera M, Valeyre D, Grenier P, et al. Sarcoidosis with pulmonary fibrosis: CT patterns and correlation with pulmonary function. AJR Am J Roentgenol 2000;174: 1751–1757
45. Bergin CJ, Bell DY, Coblentz CL, et al. Sarcoidosis: correlation of pulmonary parenchymal pattern at CT with results of pulmonary function tests. Radiology 1989;171: 619–624
46. Müller NL, Mawson JB, Mathieson JR, et al. Sarcoidosis: correlation of extent of disease at CT with clinical, functional, and radiographic findings. Radiology 1989;171: 613–618
47. Brauner MW, Grenier P, Mompoint D, et al. Pulmonary sarcoidosis: evaluation with high-resolution CT. Radiology 1989;172:467–471
48. Hansell DM, Milne DG, Wilsher ML, et al. Pulmonary sarcoidosis: morphologic associations of airflow obstruction at thin-section CT. Radiology 1998;209:697–704
49. Davies CW, Tasker AD, Padley SP, et al. Air trapping in sarcoidosis on computed tomography: correlation with lung function. Clin Radiol 2000;55:217–221
50. Magkanas E, Voloudaki A, Bouros D, et al. Pulmonary sarcoidosis: correlation of expiratory high-resolution CT findings with inspiratory patterns and pulmonary function tests. Acta Radiol 2001;42:494–501
51. Drent M, De Vries J, Lenters M, et al. Sarcoidosis: assessment of disease severity using HRCT. Eur Radiol 2003;13:2462–2471
52. Terasaki H, Fujimoto K, Muller NL, et al. Pulmonary sarcoidosis: comparison of findings of inspiratory and expiratory high-resolution CT and pulmonary function tests between smokers and nonsmokers. AJR Am J Roentgenol 2005;185:333–338
53. Akira M, Kozuka T, Inoue Y, Sakatani M. Long-term follow-up CT scan evaluation in patients with pulmonary sarcoidosis. Chest 2005;127:185–191
54. Hamper UM, Fishman EK, Khouri NF, et al. Typical and atypical CT manifestations of pulmonary sarcoidosis. J Comput Assist Tomogr 1986;10:928–936
55. Müller NL, Kullnig P, Miller RR. The CT findings of pulmonary sarcoidosis: analysis of 25 patients. AJR Am J Roentgenol 1989;152:1179–1182
56. Lenique F, Brauner MW, Grenier P, et al. CT assessment of bronchi in sarcoidosis: endoscopic and pathologic correlations. Radiology 1995;194:419–423
57. Sider L, Horton ES Jr. Hilar and mediastinal adenopathy in sarcoidosis as detected by computed tomography. J Thorac Imaging 1990;5:77–80
58. Gawne-Cain ML, Hansell DM. The pattern and distribution of calcified mediastinal lymph nodes in sarcoidosis and tuberculosis: a CT study. Clin Radiol 1996;51:263–267
59. Patil SN, Levin DL. Distribution of thoracic lymphadenopathy in sarcoidosis using computed tomography. J Thorac Imaging 1999;14:114–117
60. Niimi H, Kang EY, Kwong JS, et al. CT of chronic infiltrative lung disease: prevalence of mediastinal lymphadenopathy. J Comput Assist Tomogr 1996;20:305–308
61. Wells A. High resolution computed tomography in sarcoidosis: a clinical perspective. Sarcoidosis Vasc Diffuse Lung Dis 1998;15:140–146
62. Lynch JP III. Computed tomographic scanning in sarcoidosis. Semin Respir Crit Care Med 2003;24:393–418
63. Nishimura K, Itoh H, Kitaichi M, et al. Pulmonary sarcoidosis: correlation of CT and histopathologic findings. Radiology 1993;189:105–109
64. Honda O, Johkoh T, Ichikado K, et al. Comparison of high resolution CT findings of sarcoidosis, lymphoma, and lymphangitic carcinoma: is there any difference of involved interstitium? J Comput Assist Tomogr 1999;23: 374–379
65. Nakatsu M, Hatabu H, Morikawa K, et al. Large coalescent parenchymal nodules in pulmonary sarcoidosis: "sarcoid galaxy" sign. AJR Am J Roentgenol 2002;178:1389–1393
66. Remy-Jardin M, Giraud F, Remy J, et al. Importance of ground-glass attenuation in chronic diffuse infiltrative lung disease: pathologic-CT correlation. Radiology 1993;189: 693–698
67. Gleeson FV, Traill ZC, Hansell DM. Evidence of expiratory CT scans of small-airway obstruction in sarcoidosis. AJR Am J Roentgenol 1996;166:1052–1054

68. Bartz RR, Stern EJ. Airways obstruction in patients with sarcoidosis: expiratory CT scan findings. J Thorac Imaging 2000;15:285–289
69. Fazzi P, Sbragia P, Solfanelli S, et al. Functional significance of the decreased attenuation sign on expiratory CT in pulmonary sarcoidosis: report of four cases. Chest 2001;119:1270–1274
70. Nishino M, Kuroki M, Roberts DH, et al. Bronchomalacia in sarcoidosis: evaluation on volumetric expiratory high-resolution CT of the lung. Acad Radiol 2005;12:596–601
71. Dalal PU, Hansell DM. High-resolution computed tomography of the lungs: the borderlands of normality. Eur Radiol 2006;16:771–780
72. Aye M, Campbell AP, Greenstone MA. An unusual case of lobar collapse. Chest 2002;122:1465–1466
73. Nunes H, Humbert M, Capron F, et al. Pulmonary hypertension associated with sarcoidosis: mechanisms, haemodynamics and prognosis. Thorax 2006;61:68–74
74. Narayan D, Brown L, Thayer JO. Surgical management of superior vena caval syndrome in sarcoidosis. Ann Thorac Surg 1998;66:946–948
75. Cappell MS. Endoscopic, radiographic, and manometric findings in dysphagia associated with sarcoid due to extrinsic esophageal compression from subcarinal lymphadenopathy. Am J Gastroenterol 1995;90:489–492
76. Tobias JK, Santiago SM, Williams AJ. Sarcoidosis as a cause of left recurrent laryngeal nerve palsy. Arch Otolaryngol Head Neck Surg 1990;116:971–972
77. Jarman PR, Whyte MK, Sabroe I, Hughes JM. Sarcoidosis presenting with chylothorax. Thorax 1995;50:1324–1325
78. Johkoh T, Ikezoe J, Takeuchi N, et al. CT findings in "pseudoalveolar" sarcoidosis. J Comput Assist Tomogr 1992;16:904–907
79. Liebow AA, The J. Burns Amberson lecture: pulmonary angiitis and granulomatosis. Am Rev Respir Dis 1973; 108:1–18
80. Quaden C, Tillie-Leblond I, Delobbe A, et al. Necrotising sarcoid granulomatosis: clinical, functional, endoscopical and radiological evaluations. Eur Respir J 2005;26:778–785
81. Mackie B, Humphrey DA, Flannery MT. Atypical sarcoidosis: a case report and literature review. Am J Med Sci 2006;331:277–279
82. Ozseker ZF, Yilmaz A, Bayramgurler B, et al. Cavitary sarcoidosis: analysis of two cases. Respirology 2002;7:289–291
83. Froudarakis ME, Bouros D, Voloudaki A, et al. Pneumothorax as a first manifestation of sarcoidosis. Chest 1997;112:278–280
84. Ichikawa Y, Fujimoto K, Shiraishi T, et al. Primary cavitary sarcoidosis: high-resolution CT findings. AJR Am J Roentgenol 1994;163:745
85. Flora G, Dostanic D, Jakovic R, et al. Pneumothorax in sarcoidosis. Sarcoidosis 1991;8:75–79
86. Padley SP, Padhani AR, Nicholson A, et al. Pulmonary sarcoidosis mimicking cryptogenic fibrosing alveolitis on CT. Clin Radiol 1996;51:807–810
87. Gruden JF, Webb WR, Naidich DP, McGuinness G. Multinodular disease: anatomic localization at thin-section CT-multireader evaluation of a simple algorithm. Radiology 1999;210:711–720
88. Tsiodras S, Eiger G, Guttentag A, Lippmann M. Sarcoidosis presenting as unilateral alveolar consolidation. Am J Med Sci 1997;314:346–347
89. Gotway MB, Tchao NK, Leung JWT, et al. Sarcoidosis presenting as an enlarging solitary pulmonary nodule. J Thorac Imaging 2001;16:117–122
90. Judson MA, Uflacker R. Treatment of a solitary pulmonary sarcoidosis mass by CT-guided direct intralesional injection of corticosteroid. Chest 2001;120:316–317
91. Ito A, Fujino M, Isada A, et al. Retrograde radiographic development in pulmonary sarcoidosis. Intern Med 2006;45:819–822
92. Marten K, Rummeny EJ, Engelke C. The CT halo: a new sign in active pulmonary sarcoidosis. Br J Radiol 2004;77: 1042–1045
93. Marlow TJ, Krapiva PI, Schabel SI, et al. The "fairy ring": a new radiographic finding in sarcoidosis. Chest 1999;115: 275–276
94. Weinstein DS. Pulmonary sarcoidosis: calcified micronodular pattern simulating pulmonary alveolar microlithiasis. J Thorac Imaging 1999;14:218–220
95. Szwarcberg JB, Glajchen N, Teirstein AS. Pleural involvement in chronic sarcoidosis detected by thoracic CT scanning. Sarcoidosis Vasc Diffuse Lung Dis 2005;22:58–62
96. Kaiser PK, Lowder CY, Sullivan P, et al. Chest computerized tomography in the evaluation of uveitis in elderly women. Am J Ophthalmol 2002;133:499–505
97. Hennebicque AS, Nunes H, Brillet PY, et al. CT findings in severe thoracic sarcoidosis. Eur Radiol 2005;15:23–30
98. Wollschlager C, Khan F. Aspergillomas complicating sarcoidosis: a prospective study in 100 patients. Chest 1984;86:585–588
99. Franquet T, Muller NL, Gimenez A, et al. Spectrum of pulmonary aspergillosis: histologic, clinical, and radiologic findings. Radiographics 2001;21:825–837
100. Shorr AF, Helman DL, Davies DB, Nathan SD. Pulmonary hypertension in advanced sarcoidosis: epidemiology and clinical characteristics. Eur Respir J 2005;25:783–788
101. Battesti J-P, Georges R, Basset F, Saumon G. Chronic cor pulmonale in pulmonary sarcoidosis. Thorax 1978;33:76–84
102. Damuth TE, Bower JS, Cho K, Dantzker DR. Major pulmonary artery stenosis causing pulmonary hypertension in sarcoidosis. Chest 1980;78:888–891
103. Smith LJ, Lawrence JB, Katzenstein AL. Vascular sarcoidosis: a rare cause of pulmonary hypertension. Am J Med Sci 1983;285:38–44
104. Hoffstein V, Ranganathan N, Mullen JBM. Sarcoidosis simulating pulmonary veno-occlusive disease. Am Rev Respir Dis 1986;134:809–811
105. Barst RJ, Ratner SJ. Sarcoidosis and reactive pulmonary hypertension. Arch Intern Med 1985;145:2112–2114
106. Craig DA, Colletti PM, Ratto D, et al. MRI findings in pulmonary sarcoidosis. Magn Reson Imaging 1988;6:567–573
107. Mendelson DS, Gray CE, Teirstein AS. Magnetic resonance findings in sarcoidosis of the thorax. Magn Reson Imaging 1992;10:523–529
108. McFadden RG, Carr TJ, Wood TE. Proton magnetic resonance imaging to stage activity of interstitial lung disease. Chest 1987;92:31–39
109. Muller NL, Mayo JR, Zwirewich CV. Value of MR imaging in the evaluation of chronic infiltrative lung diseases: comparison with CT. AJR Am J Roentgenol 1992;158: 1205–1209

110. Primack SL, Mayo JR, Hartman TE, et al. MRI of infiltrative lung disease: comparison with pathologic findings. J Comput Assist Tomogr 1994;18:233–238
111. Gaeta M, Blandino A, Scribano E, et al. Chronic infiltrative lung diseases: value of gadolinium-enhanced MRI in the evaluation of disease activity–early report. Chest 2000;117: 1173–1178
112. Mana J. Magnetic resonance imaging and nuclear imaging in sarcoidosis. Curr Opin Pulm Med 2002;8:457–463
113. Jacobs MP, Baughman RP, Hughes J, Fernandez-Ulloa M. Radioaerosol lung clearance in patients with active pulmonary sarcoidosis. Am Rev Respir Dis 1985;131:687–689
114. Dusser DJ, Collignon MA, Stanislas-Leguern G, et al. Respiratory clearance of 99mTc-DTPA and pulmonary involvement in sarcoidosis. Am Rev Respir Dis 1986;134: 493–497
115. Thunberg S, Larsson K, Eklund A, Blaschke E. 99mTc-DTPA clearance measured by a dual head gamma camera in healthy subjects and patients with sarcoidosis: studies of reproducibility and relation to bronchoalveolar lavage findings. Eur J Nucl Med 1989;15:71–77
116. Chinet T, Dusser D, Labrune S, et al. Lung function declines in patients with pulmonary sarcoidosis and increased respiratory epithelial permeability to 99mTc-DTPA. Am Rev Respir Dis 1990;141:445–449
117. Bradvik I, Wollmer P, Evander E, et al. Different kinetics of lung clearance of technetium-99m labelled diethylene triamine penta-acetic acid in patients with sarcoidosis and smokers. Eur J Nucl Med 1994;21:1218–1222
118. Bradvik I, Wollmer P, Evander E, et al. One year follow-up of lung clearance of 99mTc-diethylene triamine penta-acetic acid and disease activity in sarcoidosis. Sarcoidosis Vasc Diffuse Lung Dis 2000;17:281–287
119. Bradvik I, Wollmer P, Evander E, et al. Kinetics of lung clearance of 99mTc-DTPA in smoking patients with sarcoidosis compared to healthy smokers. Respir Med 2002; 96:317–321
120. Hoitsma E, Faber CG, Drent M, Sharma OP. Neurosarcoidosis: a clinical dilemma. Lancet Neurol 2004;3:397–407
121. Smith JK, Matheus MG, Castillo M. Imaging manifestations of neurosarcoidosis. AJR Am J Roentgenol 2004; 182:289–295
122. Christoforidis GA, Spickler EM, Recio MV, Mehta BM. MR of CNS sarcoidosis: correlation of imaging features to clinical symptoms and response to treatment. AJNR Am J Neuroradiol 1999;20:655–669
123. Hayes WS, Sherman JL, Stern BJ, et al. MR and CT evaluation of intracranial sarcoidosis. AJR Am J Roentgenol 1987;149:1043–1049
124. Sherman JL, Stern BJ. Sarcoidosis of the CNS: comparison of unenhanced and enhanced MR images. AJR Am J Roentgenol 1990;155:1293–1301
125. Seltzer S, Mark AS, Atlas SW. CNS sarcoidosis: evaluation with contrast-enhanced MR imaging. AJNR Am J Neuroradiol 1991;12:1227–1233
126. Dumas JL, Valeyre D, Chapelon-Abric C, et al. Central nervous system sarcoidosis: follow-up at MR imaging during steroid therapy. Radiology 2000;214:411–420
127. Lexa FJ, Grossman RI. MR of sarcoidosis in the head and spine: spectrum of manifestations and radiographic response to steroid therapy. AJNR Am J Neuroradiol 1994;15:973–982
128. Junger SS, Stern BJ, Levine SR, et al. Intramedullary spinal sarcoidosis: clinical and magnetic resonance imaging characteristics. Neurology 1993;43:333–337
129. Pickuth D, Heywang-Kobrunner SH. Neurosarcoidosis: evaluation with MRI. J Neuroradiol 2000;27:185–188
130. Koike H, Misu K, Yasui K, et al. Differential response to corticosteroid therapy of MRI findings and clinical manifestations in spinal cord sarcoidosis. J Neurol 2000;247:544–549
131. Doughan AR, Williams BR. Cardiac sarcoidosis. Heart 2006;92:282–288
132. Nakazawa A, Ikeda K, Ito Y, et al. Usefulness of dual 67Ga and 99mTc-sestamibi single-photon-emission CT scanning in the diagnosis of cardiac sarcoidosis. Chest 2004;126: 1372–1376
133. Barneveld PC, van Leeuwen C, van Isselt JW. Scintigraphic demonstration of myocardial sarcoidosis: the added value of single-photon emission computed tomography. J Nucl Cardiol 1997;4:256–257
134. Vignaux O. Cardiac sarcoidosis: spectrum of MRI features. AJR Am J Roentgenol 2005;184:249–254
135. Shimada T, Shimada K, Sakane T, et al. Diagnosis of cardiac sarcoidosis and evaluation of the effects of steroid therapy by gadolinium-DTPA-enhanced magnetic resonance imaging. Am J Med 2001;110:520–527
136. Vignaux O, Dhote R, Duboc D, et al. Detection of myocardial involvement in patients with sarcoidosis applying T2-weighted, contrast-enhanced, and cine magnetic resonance imaging: initial results of a prospective study. J Comput Assist Tomogr 2002;26:762–767
137. Vignaux O, Dhote R, Duboc D, et al. Clinical significance of myocardial magnetic resonance abnormalities in patients with sarcoidosis: a 1-year follow-up study. Chest 2002; 122:1895–1901
138. Skold CM, Larsen FF, Rasmussen E, et al. Determination of cardiac involvement in sarcoidosis by magnetic resonance imaging and Doppler echocardiography. J Intern Med 2002;252:465–471
139. Smedema JP, Snoep G, van Kroonenburgh MP, et al. Evaluation of the accuracy of gadolinium-enhanced cardiovascular magnetic resonance in the diagnosis of cardiac sarcoidosis. J Am Coll Cardiol 2005;45:1683–1690
140. Tadamura E, Yamamuro M, Kubo S, et al. Effectiveness of delayed enhanced MRI for identification of cardiac sarcoidosis: comparison with radionuclide imaging. AJR Am J Roentgenol 2005;185:110–115
141. Smedema JP, Snoep G, van Kroonenburgh MP, et al. The additional value of gadolinium-enhanced MRI to standard assessment for cardiac involvement in patients with pulmonary sarcoidosis. Chest 2005;128:1629–1637
142. Yamagishi H, Shirai N, Takagi M, et al. Identification of cardiac sarcoidosis with (13)N-NH(3)/(18)F-FDG PET. J Nucl Med 2003;44:1030–1036
143. Okumura W, Iwasaki T, Toyama T, et al. Usefulness of fasting 18F-FDG PET in identification of cardiac sarcoidosis. J Nucl Med 2004;45:1989–1998
144. Ishimaru S, Tsujino I, Takei T, et al. Focal uptake on 18F-fluoro-2-deoxyglucose positron emission tomography images indicates cardiac involvement of sarcoidosis. Eur Heart J 2005;26:1538–1543
145. Kaminaga T, Takeshita T, Yamauchi T, et al. The role of iodine-123-labeled 15-(p-iodophenyl)-3R,S-methylpentadecanoic acid scintigraphy in the detection of local

myocardial involvement of sarcoidosis. Int J Cardiol 2004;94:99–103
146. Hyodo E, Hozumi T, Takemoto Y, et al. Early detection of cardiac involvement in patients with sarcoidosis by a non-invasive method with ultrasonic tissue characterisation. Heart 2004;90:1275–1280
147. Kanao S, Tadamura E, Yamamuro M, et al. Demonstration of cardiac involvement of sarcoidosis by contrast-enhanced multislice computed tomography and delayed-enhanced magnetic resonance imaging. J Comput Assist Tomogr 2005;29:745–748
148. Sulavik SB, Spencer RP, Weed DA, et al. Recognition of distinctive patterns of gallium-67 distribution in sarcoidosis. J Nucl Med 1990;31:1909–1914
149. Israel HL, Albertine KH, Park CH, Patrick H. Whole-body gallium 67 scans: role in diagnosis of sarcoidosis. Am Rev Respir Dis 1991;144:1182–1186
150. Sulavik SB, Spencer RP, Palestro CJ, et al. Specificity and sensitivity of distinctive chest radiographic and/or 67Ga images in the noninvasive diagnosis of sarcoidosis. Chest 1993;103:403–409
151. Sulavik SB, Spencer RP, Weed DA, et al. Recognition of distinctive patterns of gallium-67 distribution in sarcoidosis. J Nucl Med 1990;31:1909–1914
152. Line BR, Hunninghake GW, Keogh BA, et al. Gallium-67 scanning to stage the alveolitis of sarcoidosis: correlation with clinical studies, pulmonary function tests and bronchoalveolar lavage. Am Rev Respir Dis 1981;123:440–446
153. Fajman WA, Greenwald LV, Staton G, et al. Assessing the activity of sarcoidosis: quantitative 67Ga-citrate imaging. AJR Am J Roentgenol 1984;142:683–688
154. Alberts C, van der Schoot JB, van Daatselaar JJ, et al. 67Ga scintigraphy, serum lysozyme and angiotensin-converting enzyme in pulmonary sarcoidosis. Eur J Respir Dis 1983;64: 38–46
155. Beaumont D, Herry JY, Sapene M, et al. Gallium-67 in the evaluation of sarcoidosis: correlations with serum angiotensin-converting enzyme and bronchoalveolar lavage. Thorax 1982;37:11–18
156. Kohn H, Klech H, Kummer F, Mostbeck A. Assessment of activity in Sarcoidosis: sensitivity and specificity of 67-Gallium scintigraphy, serum ACE levels, chest roentgenography and blood lymphocyte subpopulations. Chest 1982; 82:732–738
157. Duffy GJ, Thirumurthi K, Casey M, et al. Semi-quantitative gallium-67 lung scanning as a measure of the intensity of alveolitis in pulmonary sarcoidosis. Eur J Nucl Med 1986;12:187–191
158. Brudin LH, Valind SO, Rhodes CG, et al. Fluorine-18 deoxyglucose uptake in sarcoidosis measured with positron emission tomography. Eur J Nucl Med 1994;21:297–305
159. Yamada Y, Uchida Y, Tatsumi K, et al. Fluorine-18-fluorodeoxyglucose and carbon-11-methionine evaluation of lymphadenopathy in sarcoidosis. J Nucl Med 1998;39:1160–1166